

Gap symmetry and charge density excitations in high- T_c superconductors with extended saddle points in electron spectrum

E.A.Pashitskii, V.I.Pentegov, A.V.Semenov

Institute of Physics, National Academy of Sciences of Ukraine,
252650, Kiev, Ukraine

Received June 25, 1998

It is shown that the strong anisotropy of the one-particle electron spectrum, due to the presence of extended saddle-point features (ESPF) close to the Fermi level in the hole-type cuprates YBCO and BSCCO, leads to the occurrence of a low-frequency peak in the spectral function of the charge density fluctuations due to the presence of acoustic plasmon branch in the collective electron spectrum. The retarded anisotropic electron-plasmon interaction leads to the suppression of the static screened Coulomb repulsion for small transferred momenta and, consequently, to the effective attraction between electrons in the $d_{x^2-y^2}$ -wave channel of the Cooper pairing of current carriers. Breaking of C_{4v} symmetry in YBCO crystals leads to a possibility of a change of $d_{x^2-y^2}$ -wave symmetry of the gap to a mixed $s-d$ gap symmetry for singlet Cooper pairs or to a p -wave gap symmetry for triplet pairs.

Key words: *extended saddle point, acoustic plasmon, d -wave pairing*

PACS: 74.20.-z, 74.72.-h, 74.72.Hs

1. Introduction

Any theoretical model intended for adequately describing the nature of the HTS in cuprates, should account for the d -wave superconducting gap symmetry, manifested by spontaneous Josephson currents [1], by generating the half-integer quanta of the magnetic flux [2,3], as well as by a strong anisotropy of the gap in the plane of CuO_2 layers [4].

One of the Cooper pairing mechanisms, producing the d -wave symmetry of the superconducting gap in high- T_c superconductors, is described by the model of the electron-magnon interaction in an almost antiferromagnetic quasi-2D Fermi liquid [5,6]. This model leads to an anisotropic repulsion between electrons (or holes) in the

entire 2D momentum space with peaks in the corners of the Brillouin zone (BZ). Such an interaction results in an effective attraction responsible for $d_{x^2-y^2}$ -wave singlet Cooper pairing. However, the main question regarding the sufficiently large value of the coupling constant of electron-magnon interaction for obtaining a high value (~ 100 K) of the critical temperature remains open.

New and important information about the structure of the electronic spectrum of high- T_c superconductors was recently obtained using the angle-resolved photoemission spectroscopy with high energy resolution [7,8]. These experiments exhibited the presence of extended saddle point features (ESPF) near the Fermi level in cuprates with hole-type conductivity. According to [9,10], the ESPF in the band spectrum can be the result of a strong hybridization of the overlapping broad and narrow 2D bands in the layered cuprate crystals.

In this paper we present results of our theoretical and numerical investigations of the effect of the ESPF in the band spectrum on the HTS mechanisms in the layered crystals of cuprates. We consider the ESPF effects on the spectrum of the collective charge-density excitations, on the screened Coulomb interaction as well as on the superconducting gap symmetry.

In §2 it is shown that the strong anisotropy of the one-particle electron spectrum in the CuO_2 layers due to the presence of ESPF leads to the occurrence of the low frequency branch with an acoustic dispersion in the collective spectrum of the electron density excitations. These excitations are similar to acoustic plasmons (AP) in metals having a multiply-connected Fermi surface (FS) with essentially different effective masses of the current carriers in different extrema of the band spectra [11,12]. The spectral function of the charge-density excitations is strongly anisotropic in this case and is peaked at frequencies corresponding to the AP branch. Due to the Kramers-Kronig relations for the reciprocal dielectric function, the static screened Coulomb interaction has got an anisotropic structure with the pronounced minimum in the region of small transferred momenta $|\mathbf{q}| \ll \pi/a$ (where a is the lattice constant). This suppression of the Coulomb repulsion is caused by a retarded interaction between electrons due to the exchange of virtual AP.

In §3 we argue that the deep minimum of the screened Coulomb repulsion due to the electron-plasmon interaction leads to the effective attraction between electrons in the $d_{x^2-y^2}$ -wave channel of the singlet Cooper pairing with the gap $\Delta_d(\varphi) \propto \cos 2\varphi$. This mechanism of the d -wave pairing differs from those proposed by the authors of [5,6], who accentuated the important role of the sharp repulsion peak at $\mathbf{q} = (\pi, \pi)$ and believed the peculiarities of the interaction at small \mathbf{q} to be irrelevant.

Breaking of the C_{4v} symmetry occurs in $YBCO$ crystals as well due to the existence of ordered 1D CuO chains along the b -axis, leading to the mixed $s + d_{x^2-y^2}$ or $s + d_{xy}$ symmetry of the gap parameter for singlet Cooper pairing, as well as to the possibility of the p -wave gap symmetry with $\Delta_p(\varphi) \propto \sin \varphi$ or $\Delta_p(\varphi) \propto \cos \varphi$ in the triplet pairing channel.

2. Acoustic plasmons and screened Coulomb interaction in crystals with ESPF

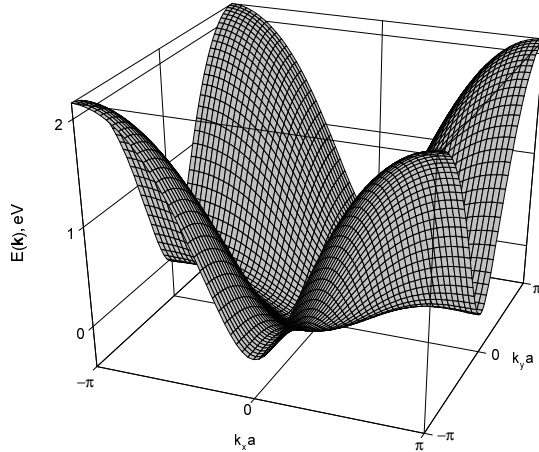


Figure 1. The conductivity band $E(k_x, k_y)$ of the 2D electron hybrid spectrum, calculated in [9].

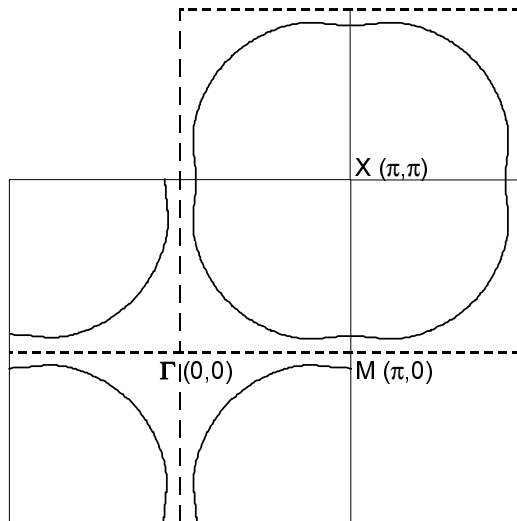


Figure 2. Cross section of the Fermi surface in the original and shifted Brillouin zones.

It is known [11,12] that a low-frequency AP branch in the collective electron spectrum can occur in multi-band (multi-valley) crystals having a multiply-connected FS and several groups of current carriers (electrons, holes) with significantly different effective masses. We show that a similar collective electron branch with acoustic dispersion relation can occur in layered crystals having a singly-connected FS but strong anisotropy in the electron density of states (DOS) and the Fermi velocity due to the presence of the ESPF [7,8]. The experimental values of the Fermi energy and Fermi momentum for the quasi-1D spectrum near the bottom of ESPF are respectively $\mu_1 \approx 20\text{meV}$ and $k_{F1} \approx 0.15\text{\AA}^{-1}$. In the parabolic spectrum approximation $\mu_1 = k_{F1}^2/2m_1^*$ we obtain an effective electronic mass $m_1^* \approx 4.3m_0$ (where m_0 is the bare electron mass).

In the present paper when choosing parameters for the hybridized conductivity band we use the results of the multiple band calculations of [9]. This conductivity band $E(k_x, k_y)$ is shown in figure 1. When the Fermi level lies above the bottom of the ESPF, it is convenient to use a shifted BZ centered in (π, π) point, in order to obtain a closed hole-type FS (figure 2).

We proceed to show that the strong anisotropy of the DOS on the FS (and hence the anisotropy of the Fermi velocity of the quasi-particles) leads to the occurrence of the low frequency AP branch in the collective electron spectrum, despite the fact that the FS is singly connected.

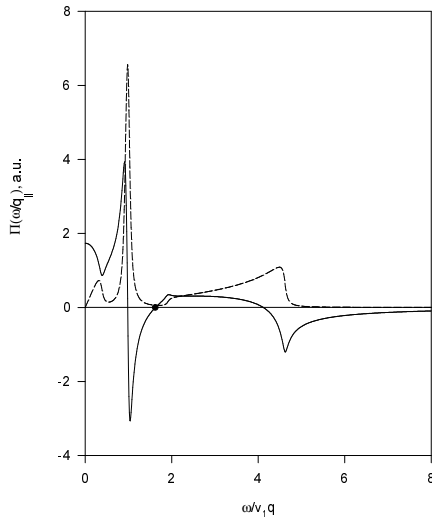


Figure 3. The real (solid curve) and imaginary (dashed curve) parts of the polarization operator in the long wave limit ($q \rightarrow 0$), when q is parallel to one of the main crystallographic axes, in a function of $\frac{\omega}{v_1 q_{\parallel}}$ for the case of strong anisotropy of the Fermi velocity.

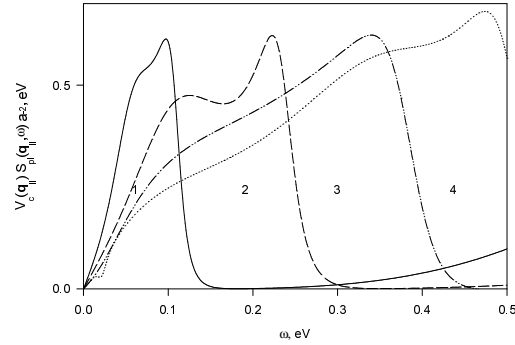


Figure 4. The frequency dependence of the spectral function of the electronic charge density fluctuations $S_{pl}(\mathbf{q}, \omega)$ multiplied by the bare Coulomb matrix element $V_c(\mathbf{q})$ for $q_{\perp} = 0$ and for several values of \mathbf{q}_{\parallel} along the BZ diagonal: 1 - $q_{\parallel} = \frac{\sqrt{2}\pi}{16a}$, 2 - $q_{\parallel} = \frac{\sqrt{2}\pi}{8a}$, 3 - $q_{\parallel} = \frac{3\sqrt{2}\pi}{16a}$, 4 - $q_{\parallel} = \frac{\sqrt{2}\pi}{4a}$.

The dispersion relation $\omega_{pl}(q)$ of the AP branch is determined by zero of the real part of the longitudinal complex dielectric function

$$\varepsilon(\mathbf{q}, \omega) = 1 + V_c(\mathbf{q}) \Pi(\mathbf{q}_{\parallel}, \omega), \quad (1)$$

where V_c is the matrix element of the Coulomb interaction in the layered crystals,

$$V_c(\mathbf{q}) = \frac{2\pi e^2}{q_{\parallel}} \cdot \frac{\sinh q_{\parallel} d}{\cosh q_{\parallel} d - \cos q_{\perp} d} \quad (2)$$

and Π is the polarization operator, corresponding to the 2D band $E(\mathbf{k}_{\parallel})$, which is crossed by the Fermi level. Here \mathbf{q}_{\parallel} and \mathbf{k}_{\parallel} are the longitudinal momenta in the $a-b$ plane, q_{\perp} is the transverse momentum along the c -axis, d is the distance between layers.

In figure 3 the real and imaginary parts of the polarization operator are shown as functions of ω/q_{\parallel} for $q_{\parallel} \rightarrow 0$.

The spectral function of the electronic charge density fluctuations (virtual plasmons) given by

$$S_{pl}(\mathbf{q}, \omega) = -\frac{1}{\pi} \text{Im} \varepsilon^{-1}(\mathbf{q}, \omega) = \frac{1}{\pi} \frac{\text{Im} \varepsilon(\mathbf{q}, \omega)}{[\text{Re} \varepsilon(\mathbf{q}, \omega)]^2 + [\text{Im} \varepsilon(\mathbf{q}, \omega)]^2} \quad (3)$$

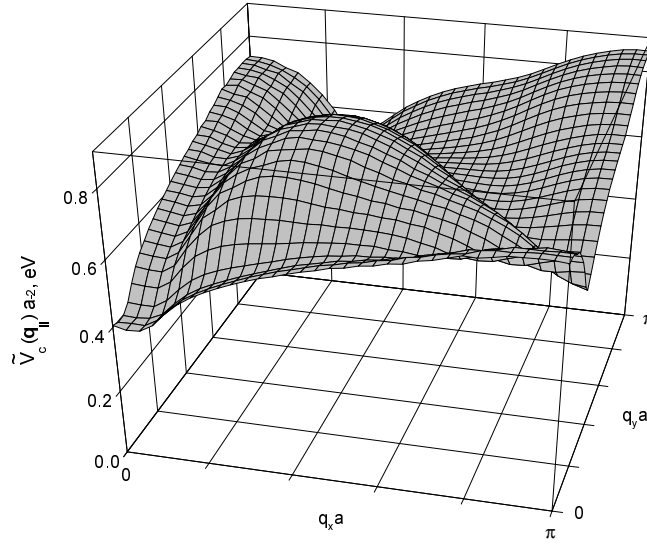


Figure 5. The plot of the static screened Coulomb repulsion $\tilde{V}_c(\mathbf{q}_{\parallel})$ calculated for the electron spectrum of figure 1.

and calculated with the electron spectrum of figure 1, is plotted in figure 4 for several $\mathbf{q}_{\parallel} \neq \mathbf{0}$ along one of the two BZ diagonals and for $q_{\perp} = 0$. The function $S_{\text{pl}}(\mathbf{q}, \omega)$ has got a maximum at the frequency $\omega_{\text{pl}}(q)$ of the AP since $\text{Re} \varepsilon(\mathbf{q}, \omega_{\text{pl}}) = \mathbf{0}$, while for $\omega \rightarrow 0$ according to (3) $S_{\text{pl}}(\mathbf{q}, \omega) \sim \omega$ since $\text{Im} \varepsilon(\mathbf{q}, \omega) \sim \omega$.

By virtue of the Kramers-Kronig relation for the reciprocal dielectric function $\varepsilon^{-1}(\mathbf{q}, \omega)$ the matrix element of the static (for $\omega = 0$) screened Coulomb repulsion between electrons can be written as

$$\tilde{V}_c(\mathbf{q}) \equiv \frac{V_c(\mathbf{q})}{\varepsilon(\mathbf{q}, \mathbf{0})} = V_c(\mathbf{q}) \left[1 - 2 \int_0^{\infty} \frac{d\omega'}{\omega'} S_{\text{pl}}(\mathbf{q}, \omega') \right]. \quad (4)$$

The plot of $\tilde{V}_c(\mathbf{q}_{\parallel})$ calculated for the band of figure 1 is presented in figure 5. As we see, $\tilde{V}_c(\mathbf{q})$ has got a deep minimum in the region of small transferred momenta \mathbf{q}_{\parallel} due to the low frequency maximum of the charge density spectral function $S(\mathbf{q}, \omega)$ in the region of the AP branch presence. Such a suppression of the static Coulomb repulsion is caused by the effective electron-electron attraction through the exchange of the virtual AP.

In the general case of C_{4v} symmetry of the electron spectrum the Fourier series expansion of the screened Coulomb matrix element $\tilde{V}_c(\mathbf{k}_{\parallel} - \mathbf{k}'_{\parallel})$ with respect to the angles φ and φ'

$$\tilde{V}_c(\varphi, \varphi') = \sum_{n,m} V_{nm} e^{in\varphi + im\varphi'}. \quad (5)$$

will contain harmonics V_{nm} with indices satisfying the condition $n + m = 4l$, where l is an integer.

3. The effect of the electron spectrum anisotropy on the gap symmetry

In what follows, we show that the marked momentum dependence of the screened Coulomb interaction (4), connected to the low frequency peak of the plasmon spectral function (3), determines the symmetry of the superconducting gap.

We will use the Eliashberg equations [13] for the gap in superconductors with strong coupling, taking into account the retarded interaction between electrons due to the exchange of virtual phonons and acoustic plasmons, as well as the screened Coulomb repulsion. Near the critical temperature, $T \rightarrow T_c$, the linearized equation for the anisotropic gap $\Delta(\mathbf{k}_{\parallel}, \omega)$ on the FS, given the quasi-2D character of the electron spectrum, using the static Kramers-Kronig relation (4), can be written on the FS ($|\mathbf{k}_{\parallel}| = k_F$) as

$$(1 + \lambda) \Delta(\varphi, 0) = \frac{1}{2} \int_0^{2\pi} \frac{d\varphi'}{2\pi} \int_{-\tilde{\Omega}}^{\tilde{\Omega}} \frac{d\omega}{\omega} \Delta(\varphi', \omega) \nu(\varphi', \omega) \times \left[W_{\text{ph}} \theta(\tilde{\Omega}_{\text{ph}} - |\omega|) - \tilde{V}_c(\varphi, \varphi') \right] \tanh \frac{\omega}{2T_c}, \quad (6)$$

where λ is the renormalization constant, connected to the normal self-energy, $\theta(x)$ is the unit step function, the electron-phonon interaction W_{ph} is taken to be quasi isotropic, $\tilde{\Omega}$ is a cut-off energy of the Coulomb interaction ($\tilde{\Omega} \approx E_F$), and $\nu(\varphi', \omega)$ is the anisotropic DOS.

3.1. Unbroken C_{4v} symmetry

For the layered crystals, having the unbroken C_{4v} symmetry of the electron spectrum (for instance, BiSrCaCuO, TlBaCaCuO, HgBaCaCuO), the anisotropic DOS can be approximated by

$$\nu(\varphi, \omega) = \nu_+(\omega) + \nu_-(\omega) \cos 4\varphi, \quad (7)$$

where

$$\nu_{\pm}(\omega) = \frac{1}{2} \left[\nu_1 \operatorname{Re} \sqrt{\frac{\mu_1}{\mu_1 + \omega}} \pm \nu_2 \right]. \quad (8)$$

At the same time it is possible to retain in the Fourier expansion (5) only the main terms, corresponding to the A_1 and B_1 representations of the C_{4v} group:

$$\tilde{V}_c(\varphi, \varphi') \approx V_{00} + V_{22} (\cos 2\varphi \cos 2\varphi' - \sin 2\varphi \sin 2\varphi') + V_{44} (\cos 4\varphi \cos 4\varphi' - \sin 4\varphi \sin 4\varphi'), \quad (9)$$

where the isotropic part of the Coulomb repulsion $V_{00} > 0$, while V_{22} and V_{44} , containing the anisotropic contribution of the electron-plasmon interaction, may be either positive or negative (see below). Substituting (7) and (9) in equation (6) we conclude that the singlet Cooper pairing is possible either in d - or s -channels. For the s -wave pairing with the anisotropic gap

$$\Delta_s(\varphi) = \Delta_0 + \Delta_4 \cos(4\varphi) \quad (10)$$

we obtain the following coupled equations determining the critical temperature T_c^s

$$(1 + \lambda) \Delta_0 = \frac{W_{\text{ph}} - V_{00}^*}{2} \int_{-\tilde{\Omega}_{\text{ph}}}^{\tilde{\Omega}_{\text{ph}}} \frac{d\omega}{\omega} \left[\nu_+(\omega) \Delta_0 + \frac{\nu_-(\omega) \Delta_4}{2} \right] \tanh \frac{\omega}{2T_c^s} \quad (11)$$

$$(1 + \lambda) \Delta_4 = -\frac{1}{4} V_{44} \int_{-\tilde{\Omega}}^{\tilde{\Omega}} \frac{d\omega}{\omega} [\nu_+(\omega) \Delta_4 + \nu_-(\omega) \Delta_0] \tanh \frac{\omega}{2T_c^s}, \quad (12)$$

where

$$V_{00}^* = \frac{V_{00}}{1 + \nu_2 V_{00} \ln(E_F / \tilde{\Omega}_{\text{ph}})}. \quad (13)$$

For the d -wave pairing the critical temperature T_c^d is given by equation

$$(1 + \lambda) \cdot \Delta_d(\varphi) = -\frac{V_{22}}{2} \int_0^{2\pi} \frac{d\varphi'}{2\pi} \int_{-\tilde{\Omega}}^{\tilde{\Omega}} \frac{d\omega}{\omega} \nu(\varphi', \omega) \Delta_d(\varphi') \times (\cos 2\varphi \cos 2\varphi' - \sin 2\varphi \sin 2\varphi') \tanh \frac{\omega}{2T_c^d} \quad (14)$$

The sign of the coefficient V_{22} determines the type of d -wave symmetry of the gap. For the negative value of V_{22} the gap has $d_{x^2-y^2}$ symmetry, $\Delta_d(\varphi) = \Delta_2 \cos 2\varphi$, and the equation (14) is reduced to

$$(1 + \lambda) = \frac{|V_{22}|}{4} \int_{-\tilde{\Omega}}^{\tilde{\Omega}} \frac{d\omega}{\omega} \left(\nu_+(\omega) + \frac{1}{2} \nu_-(\omega) \right) \tanh \frac{\omega}{2T_c^d}. \quad (15)$$

For the positive value of V_{22} from (14) the solution of the form $\Delta_d(\varphi) = \Delta_2 \sin 2\varphi$ follows, corresponding to the d_{xy} -wave gap symmetry.

3.2. YBCO-type crystals with CuO chains

For the $\text{YBa}_2\text{Cu}_3\text{O}_7$ and $\text{YBa}_2\text{Cu}_4\text{O}_8$ crystals, where C_{4v} symmetry is broken due to the presence of the ordered 1D chains CuO, the anisotropic DOS has got approximately the following angular dependence

$$\nu(\varphi, \omega) = \tilde{\nu}_0(\omega) - \frac{\tilde{\nu}_c}{2} \cos 2\varphi + \nu_-(\omega) \cos 4\varphi, \quad (16)$$

where $\tilde{\nu}_0(\omega) = \nu_+(\omega) + \tilde{\nu}_c/2$, and $\tilde{\nu}_c$ is the electron DOS in the 1D chains.

The asymmetric terms in the electron-electron interaction in this case are

$$U(\varphi, \varphi') = \tilde{U}_{11} (1 + \cos \varphi \cos \varphi' - \sin \varphi \cdot \sin \varphi'). \quad (17)$$

Substitution of (16) and (17) in (6) leads, for the singlet Cooper pairing, to the system of coupled gap equations

$$(1 + \lambda) \Delta_0 = \frac{W_{\text{ph}} - \tilde{U}_{11} - V_{00}^*}{2} \int_{-\tilde{\Omega}_{\text{ph}}}^{\tilde{\Omega}_{\text{ph}}} \frac{d\omega}{\omega} \left[\Delta_0 \tilde{\nu}_0(\omega) + \frac{\Delta_2 \tilde{\nu}_c}{2} \right] \tanh \frac{\omega}{2T_c}, \quad (18)$$

$$(1 + \lambda) \Delta_2 = \frac{|V_{22}|}{4} \int_{-\tilde{\Omega}}^{\tilde{\Omega}} \frac{d\omega}{\omega} \left\{ \Delta_0 \tilde{\nu}_c + \Delta_2 \left[\tilde{\nu}_0(\omega) + \frac{\nu_-(\omega)}{2} \right] \right\} \tanh \frac{\omega}{2T_c} \quad (19)$$

for s - and d -wave components of the anisotropic superconducting gap which is given by,

$$\Delta_{sd}(\varphi) = \begin{cases} \Delta_0 + \Delta_2 \cos 2\varphi & \text{if } V_{22} < 0, \\ \Delta_0 + \Delta_2 \sin 2\varphi & \text{if } V_{22} > 0. \end{cases} \quad (20)$$

In other words, the presence of the 1D chains of CuO in YBCO should bring about the mixed s - d symmetry of the gap.

Furthermore, a sufficiently strong interaction \tilde{U}_{11} in (17), violating the C_{4v} symmetry, could give rise to triplet Cooper pairing of electrons in 1D chains with p -type order parameter symmetry

$$\Delta_p(\varphi) = \begin{cases} \Delta_1 \cos \varphi & \text{if } \tilde{U}_{11} < 0 \\ \Delta_1 \sin \varphi & \text{if } \tilde{U}_{11} > 0 \end{cases} . \quad (21)$$

In this case, the critical temperature T_c^p will be defined by the equation

$$(1 + \lambda) = \frac{1}{4} |\tilde{U}_{11}| \int_{-\tilde{\Omega}}^{\tilde{\Omega}} \frac{d\omega}{\omega} \tilde{\nu}_0(\omega) \tanh \frac{\omega}{2T_c^p}. \quad (22)$$

Notice that the negative value of \tilde{U}_{11} can result from the strong electron-phonon interaction in the CuO chains.

4. Conclusions

We have shown that strong anisotropy of the one-particle electron spectrum, associated, in particular, with the presence of the ESPF near the Fermi level, may lead to the occurrence of the acoustic plasmon branch in the collective electron spectrum. These electronic excitations cause the low frequency peak in the spectral function of the charge density fluctuations $S_{pl}(\mathbf{q}, \omega) = -\frac{1}{\pi} \text{Im} \varepsilon^{-1}(\mathbf{q}, \omega)$ and, through the Kramers-Kronig relation for the reciprocal dielectric function $\varepsilon^{-1}(\mathbf{q}, \omega)$, lead to the deep minimum in the static screened Coulomb repulsion for the small transferred momenta \mathbf{q} . Such a suppression of the Coulomb repulsion, which is the result of the effective electron-electron attraction due to the exchange of the virtual acoustic plasmons, favours the $d_{x^2-y^2}$ -wave Cooper pairing of the current carriers with the superconducting gap structure $\Delta_d(\varphi) \sim \cos 2\varphi$ in the layered crystals of the cuprate metal-oxide compounds, having C_{4v} symmetry of the CuO₂ layers. Breaking of C_{4v} symmetry leads to the mixed $s - d$ wave singlet Cooper pairing, or to the p -wave triplet pairing of current carriers.

References

1. Wollman D.A., Van Harlingen D.J., Lee W.C., Ginsberg D.M., Leggett A.J. Experimental determination of the superconducting pairing state in YBCO from the phase coherence of YBCO-Pb dc SQUIDs. // *Phys. Rev. Lett.*, 1993, vol. 71, p. 2134.
2. Tsuei S.S., Kirtley J.R., Chi C.C., Yu-Jahnes L.S., Gupta A., Shaw T., Sem J.Z., Ketchen M.B. Pairing symmetry and flux quantization in a tricrystal superconducting ring of $\text{YBa}_2\text{Cu}_3\text{O}_{7-\delta}$. // *Phys. Rev. Lett.*, 1994, vol. 73, p. 593.
3. Kirtley J.R., Tsuei S.S., Rupp M., Sun J.Z., Yu-Jahnes L.S., Gupta A., Ketchen M.B., Moler K.A., Bhushan M. Direct imaging of integer and half-integer Josephson vortices in high- T_c grain boundaries. // *Phys. Rev. Lett.*, 1996, vol. 76, p. 1336.
4. Ding H., Norman M.R., Campuzano J.C., Rnaderia M., Bellman A.F., Yokoya T., Takahashi T., Mochiku T., Kadowaki K. Angle-resolved photoemission spectroscopy study of the superconducting gap anisotropy in $\text{Bi}_2\text{Sr}_2\text{CaCu}_2\text{O}_{8+x}$. // *Phys. Rev. B*, 1996, vol. 54, p. R9678.
5. Millis A.J., Monien H., Pines D. Phenomenological model of nuclear relaxation in the normal state of $\text{YBa}_2\text{Cu}_3\text{O}_7$. // *Phys. Rev. B*, 1990, vol. 42, p. 167.
6. Pines D. $d_{x^2-y^2}$ pairing and spin fluctuations in the cuprate superconductors: experiment meets theory. // *Physica C*, 1994, vol. 235–240, p. 113;
Nearly antiferromagnetic Fermi liquids: a progress report. // *Zeit. Phys. B*, 1997, vol. 103, p. 129.
7. King D.M., Shen Z.-X., Dessau D.S., Marshall D.S., Park C.H., Spicer W.E., Peng J.L., Li Z.Y., Greene R.L. Observation of a saddle-point singularity in $\text{Bi}_2(\text{Sr}_{0.97}\text{Pr}_{0.03})_2\text{CuO}_{6+d}$ and its implications for normal and superconducting state properties. // *Phys. Rev. Lett.*, 1994, vol. 73, p. 3298.
8. Gofron K., Campuzano J.C., Abrikosov A.A., Lindroos M., Bansil A., Ding H., Koelling D., Dabrowski B. Observation of an “extended” Van Hove singularity in $\text{YBa}_2\text{Cu}_3\text{O}_8$ by ultrahigh energy resolution angle-resolved photoemission. // *Phys. Rev. Lett.*, 1994, vol. 73, p. 3302.
9. Andersen O.K., Jepsen O., Liechtenstein A.I., Mazin I.I. Plane dimpling and saddle-point bifurcation in the band structures of optimally doped high-temperature superconductors: A tight-binding model. // *Phys. Rev. B*, 1994, vol. 49, p. 4145.
10. Pashitskii E.A., Pentegov V.I. On the nature of the anisotropic gap structure in high-temperature superconductors: competition between s - and d -symmetry types. // *Zh. Eksp. Teor. Fiz.*, 1997, vol. 111, p. 298 [*JETP*, 1997, vol. 84, p. 164].
11. Pines D. Electron interaction in solids. // *Canad. J. Phys.*, 1956, vol. 34, 1379.
12. Ruvalds J. Are there acoustic plasmons? // *Adv. Phys.*, 1981, vol. 30, p. 677.
13. Eliashberg G.M. Interaction between electrons and lattice vibrations in a superconductor. // *Zh. Exsp. Teor. Fiz.*, 1960, vol. 38. p. 966 [*Sov. Phys. JETP*, 1960, vol. 11, p. 696];
Temperature Green’s functions for electrons in superconductors. // *Zh. Exsp. Teor. Fiz.*, 1960, vol. 39, p. 1437 [*Sov. Phys. JETP*, 1961, vol. 12, p. 1000].

Симетрія надпровідної щілини та збудження зарядової густини у високотемпературних надпровідниках з подовженими сідловими особливостями в електронному спектрі

Е.А.Пашицький, В.І.Пентегов, О.В.Семенов.

Інститут Фізики НАН України, 252650, Київ

Отримано 25 червня 1998 р.

Показано, що сильна анізотропія одночасткового електронного спектру веде, завдяки наявності подовжених сідлових особливостей біля рівня Фермі у купратах YBCO та BSCCO, до появи низькочастотного піку у спектральній функції флуктуацій зарядової густини, що є наслідком присутності гілки акустичних плазмонів у колективному електронному спектрі. Електрон-плазмонна взаємодія веде до значного зменшення статичного кулонівського відштовхування в області малих переданих імпульсів та, як наслідок, до ефективного притягнення між електронами у $d_{x^2-y^2}$ -хвильовому каналі куперівського спарювання носіїв струму. Порушення C_{4v} симетрії у кристалах YBCO призводить до можливості заміни $d_{x^2-y^2}$ -хвильової симетрії надпровідної щілини на змішану $s-d$ симетрію для синглетних куперівських пар або на p -хвильову симетрію щілини для триплетних пар.

Ключові слова: подовжені сідлові точки, акустичний плазмон, d -хвильове спарювання

PACS: 74.20.-z, 74.72.-h, 74.72.Hs